INSTITUTE OF PHYSICS PUBLISHING JOURNAL OF PHYSICS D: APPLIED PHYSICS

J. Phys. D: Appl. Phys. **37** (2004) 678–688 PII: S0022-3727(04)71578-8

The optical functions of metal phthalocyanines

Z T Liu[1], H S Kwok[1] and A B Djurišić[2]

[1] Department of Electrical and Electronic Engineering, Hong Kong University of Science and Technology, Clearwater Bay, Hong Kong
[2] Department of Physics, University of Hong Kong, Pokfulam Road, Hong Kong

E-mail: dalek@hkusua.hku.hk

Received 8 November 2003
Published 11 February 2004
Online at stacks.iop.org/JPhysD/37/678 (DOI: 10.1088/0022-3727/37/5/006)

Abstract

The optical properties of five metal phthalocyanines (MPcs) thin films (cobalt phthalocyanine (Pc), copper Pc, iron Pc (FePc), nickel Pc, and zinc Pc), were studied by spectroscopic ellipsometry. Thin films of these MPcs were evaporated in high vacuum onto glass substrates, quartz substrates, and silicon substrates. Spectroscopic ellipsometry measurements were performed in the wavelength range 250–800 nm. The absorption spectra were measured, and the film thickness and surface roughness were studied by atomic force microscopy. Determination of optical functions was performed by simultaneous fitting of the experimental data for samples on glass and silicon substrates. Fitting results using point-to-point fitting, the Lorentz model, the modified Lorentz model, the relaxed Lorentz model, and the dual Lorentz model were compared. Models with six oscillators were used to fit the optical functions of FePc, while five oscillators were used for the other four Pcs. It was found that modifications of the Lorentz model are more suitable for description of the optical functions of the MPcs compared with the conventional Lorentz model.

1. Introduction

Phthalocyanines (Pcs) are a common class of organic compounds. The first synthesis of Pc was reported in 1907 [1]. In 1930 the molecular structures of Pc and metal Pcs (MPcs) were found and confirmed. It was found that Pcs have many attractive properties: availability in high purity due to the ease of crystallization and sublimation; extraordinary thermal and chemical stability; attractive optical properties (intense absorption in the red and blue spectrum range, which makes them very pure blue pigments); and a large number of available compounds (there are more than 70 MPcs that are known) [2]. Because of these distinct characteristics, Pcs have been widely used as blue and green inks, as pigments for colouring plastics and metal surfaces, as dyes for clothing, and as catalysts in the oil industry [3]. In recent years, new applications have emerged for Pcs due to their semiconducting properties. They have been used in photovoltaic devices [1, 4–6], photodetectors [7], organic transistors [2, 8], organic electroluminescence devices [9–11], and sensors [12, 13]. Among small-molecule-based photovoltaic devices, the highest power conversion efficiency of 3.6% was reported for a copper Pc (CuPc)-based cell [4]. CuPc is also commonly used as a hole injection layer in organic light emitting diodes (OLEDs) [9, 10]. While the properties of CuPc are relatively well known, there are very few studies of other MPcs. It has been pointed out recently that nickel Pc (NiPc) is promising for organic photovoltaic applications [6]. Due to its relatively high hole mobility [6], it is possible that NiPc may also find application as a hole injection layer in OLEDs. Other MPcs are also of interest for photovoltaic applications [1]. Therefore, determination of their optical properties is of interest in order to model the performance of organic optoelectronic devices as well as to design devices with improved performance (which would also require determination and modelling of the charge transport properties).

The absorption and luminescent properties of MPcs have been extensively studied, and their absorption spectra have been assigned to electron orbital transitions. However, little attention has been paid to the optical functions of MPcs, which have substantial impact on the performance of the devices based on MPcs like OLEDs and organic

photovoltaics. Even less effort has been made to model their optical properties. The optical properties of MPcs are very important for understanding their molecular structure and improving the performance of devices made with MPcs. The electronic structure and optical transitions in MPcs have been studied extensively. For most MPcs, five transition bands, labelled as Q, B, N, L, and C bands, were identified, and their corresponding energies are approximately 2, 3.6, 4.4, 5.0, and 5.9 eV [14]. Some MPcs may miss one or two of these bands. The absorption spectra of MPcs have been studied in vapour form [14, 15], in solution [16], and in solid state [17–21]. Although the absorption line shapes vary from case to case, they have several common peaks (transition bands). However, while the absorption spectra of a number of MPcs have been reported, studies of their index of refraction have been scarce. Schechtman and Spicer [18] obtained the extinction coefficient from the absorption data and then calculated the refractive index from the extinction coefficient by numerical Kramers–Kronig (KK) inversion. However, this method did not take into account the reflection loss during the absorption measurements. Furthermore, the extinction coefficient beyond the measured range, which is necessary to do the KK inversion, was obtained by extrapolation, and the calculated refractive index can differ from the real value by an arbitrary constant.

Reliable values of both real and imaginary parts of the refractive index can be obtained by SE measurements, but SE studies of MPcs have been limited mainly to CuPc and cobalt Pc (CoPc) [22–27]. Moreover, these studies do not agree well with each other. Debe and Field [23, 24] studied CuPc in the range 400–800 with a 10 nm step, and the resulted extinction coefficient (k) agreed well with the measured absorption. Gu and Chen [25, 26] studied CoPc and CuPc thin films, in the range 550–800 nm with a 20 nm step, but their results are not consistent with other results reported in the literature. Point-by-point fitting was used to determine the optical functions in these studies. In our previous work [27], we reported SE measurements of CuPc in the spectral range 1.55–4.1 eV and fitted the data using point-by-point fitting and conventional and modified Lorentz models (MLMs). Modelling of SE data for MPcs and organic compounds in general has been scarce [27–31]. The models used were the conventional Lorentz model (CLM) and its modifications [27–29] and the Forouhi and Bloomer model [30]. The latter has been used to fit the index of refraction of tris(8-hydroxyquinoline) aluminium over a narrow spectral range where only one absorption peak can be observed [30]. There were attempts to fit the absorption lines of MPcs with Lorentz or Gaussian models [19]. It was found that for some of the peaks the Lorentz model is more accurate and for others the Gaussian model is better. Therefore, it is likely that the CLM is not always the best choice for fitting the optical functions of MPcs. A numerically evaluated convolution of the Gaussian and Lorentzian models was also used to model the optical properties of organic thin films [31], and the considerable inhomogeneous broadening contributions obtained were attributed to the high concentration of defects in evaporated polycrystalline Pc films.

In this work, SE was used to study the optical properties of thin films of five MPcs: CoPc, CuPc, iron Pc (FePc), NiPc, and zinc Pc (ZnPc). The film thickness and surface roughness were studied by atomic force microscopy (AFM). The optical functions were determined by simultaneous fitting of SE measurements for the thin films on glass and Si substrates. Measurements at different incident angles were performed to establish whether the samples can be considered isotropic. In addition to point-by-point fitting, the data were fitted with the CLM, the MLM, the relaxed Lorentz model (RLM), and the dual Lorentz model (DLM). The results obtained by the different models are compared and discussed. This paper is organized as follows. In section 2, the experimental details are given. In section 3, the models and data fitting procedure are described. In section 4, the results obtained are presented and discussed.

2. Experimental details

The experimental details of sample fabrication and characterization are described below.

2.1. Sample fabrication

Glass substrates with one rough surface and silicon substrates were used in the samples for SE measurements. The bottom surface of the glass substrates was made rough to suppress the reflection of incident light from the bottom surface during the SE measurements. The glass substrates were cleaned in an ultrasonic bath for 20 min in acetone, ethanol, and de-ionized (DI) water, respectively. Then the glass was washed in the ultrasonic bath for 30 min, sprayed with DI water for 10 min, soaked in DI water in ultrasonic bath for 30 min, and oven bake-dried for 1–2 h.

Lightly doped p-type Si wafers were cleaned by the standard procedure just before fabrication to prevent the growth of silicon dioxide on the surface. At first the wafers were put into DI water for the standard four-cycle dump-rinse to wet the wafer surface and remove particles. Then approximately 600 ml of H_2O_2 was added to the H_2SO_4–H_2O_2 bath. H_2O_2 acts as a bubbler that helps remove particles from the wafer surfaces since it decomposes readily into H_2O and O_2 (which causes the bubbling action). Then the wafer was immersed into the bath (10 : 1, $H_2SO_4 : H_2O_2$ at 120°C) and left for 10 min to remove organic contaminants. After another four-cycle dump-rinse in DI water to rinse off the sulfuric acid prior to the HF clean, the wafers were carefully put into the HF bath ($HF : H_2O = 1 : 50$) for 30 s to remove the oxide that was formed both in air and particularly in the sulfuric–peroxide bath. Finally, after another four-cycle dump-rinse in DI water, the wafers were put into a spin-dryer to dry.

The quartz substrates were used in the samples for absorption measurements and AFM measurements (for thickness determination). They were cleaned by the same procedure as the glass substrates. A Denton DV-502A high-vacuum evaporator was used to fabricate thin films of MPcs. MPc powder was put in a tungsten boat, with three substrates (a quartz substrate, a glass substrate, and a Si substrate) placed on the substrate holder ∼20 cm above the evaporation source. The film thickness was monitored by a quartz detector near the substrates. The deposition rate was 1 Å s^{-1}, and the pressure in the chamber was 2×10^{-6} Torr. The substrates were rotated during the deposition to enhance the thickness uniformity. The substrates were held at room temperature.

2.2. SE measurements

The SE measurements were conducted using a UVISEL spectroscopic phase modulated ellipsometer from Jobin Yvon Co. The studies on the luminescence and phosphorescence of MPcs [16, 32, 33] found very low quantum yields (10^{-2}–10^{-5}), so that the contribution of emission of the MPcs to the SE measurements can be ignored. During the measurements, the incident angle was set to 70°. For each sample, at least two points were measured, and for each point the SE data were taken from two perpendicular orientations in order to test the existence of in-plane anisotropy. Therefore four sets of data were taken for each sample to eliminate errors and to verify the isotropy of the films. The measurements were performed in the range 250–800 nm, with a wavelength interval of 2.5 nm. SE measurements with variable incident angles for NiPc were also performed with the incident angle changed from 45° to 75°, with a step of 5°, in order to test the isotropy of the films. Due to the planar structure of each individual MPc, anisotropy would be expected in case of preferential molecule orientation in the films. Later, these data were fitted using same n and k to verify the isotropy of NiPc. The fitting results show that NiPc thin films can be described as isotropic (or have very small anisotropy). This is in agreement with the study of Barrett *et al* [22], who found that CuPc films with a thickness below 80–100 nm can be considered isotropic.

2.3. Absorbance measurements

The absorbance measurements were conducted to determine the absorption spectrum of the MPcs as well as to verify the ellipsometry fitting results. A Lambda 20 UV/VIS spectrophotometer from Perkin Elmer was used for the measurement. Absorbance was measured in the range 250–1000 nm, with a resolution of 1 nm.

2.4. AFM measurements

An AFM was used to check the surface roughness of the MPc samples as well as to find out the thickness of the MPc thin films. A NanoScope scanning probe microscope, Model MultiMode, was used to perform the measurements. In order to measure the thickness of the thin films, the samples were scratched by a needle and the scratched surfaces were examined using the AFM. Quartz substrates were used in the samples for AFM measurements because of the high hardness of quartz. From the AFM images, the roughness of surfaces for all MPc films on quartz was found out to be around 2 nm.

3. Description of the model and the fitting procedure

The experimental data were first fitted using the Lorentz model, with the film thickness as one fitting parameter. The fitted thickness was verified by AFM measurements. The thickness values obtained were 48 nm for CoPc, 49 nm for CuPc, 56 nm for FePc, 45 nm for NiPc, and 36 nm for ZnPc. Then the fitted thickness was used to do the point-by-point fitting, which uses the same dielectric constants and the same thickness for both the sample on the glass substrate and the sample on the Si substrate. In such a way, the system is overdetermined, i.e. for each wavelength there are four equations to be satisfied, but only two parameters (n and k), so that the reliability of the obtained results is improved. After point-by-point fitting had been obtained, fitting with different models of the optical functions was performed. The CLM, MLM, RLM, and DLM were used.

The dielectric function in CLM is given by [27–29]

$$\varepsilon(\omega) = \varepsilon_\infty + \sum_j \frac{F_j}{\omega_j^2 - \omega^2 + \mathrm{i}\Gamma_j\omega}, \tag{1}$$

where j is the number of Lorentzian oscillators and ω_j, F_j, and Γ_j are the peak frequency, strength, and broadening of the jth oscillator, respectively.

The dielectric function defined by MLM is given by the following equations [27]

$$\varepsilon(\omega) = \varepsilon_\infty + \sum_j \frac{F_j}{\omega_j^2 - \omega^2 - \mathrm{i}\Gamma'_j\omega}, \tag{2}$$

where j is the number of Lorentzian oscillators and ω_j, F_j, and Γ'_j are the peak frequency, strength, and broadening of the jth oscillator, respectively. Unlike CLM, where the width, Γ, is a constant, in MLM, Γ'_j is a function of frequency given by [27]

$$\Gamma'_j(\omega) = \Gamma_j(\omega)\exp\left[-\alpha_j\left(\frac{|\hbar\omega| - \hbar\omega_j}{\Gamma_j}\right)\right], \tag{3}$$

where α_j is the broadening factor of the jth oscillator. If $\alpha_j = 0$, then the jth oscillator is a Lorentz oscillator. When $\alpha_j \sim 0.2$, the jth oscillator is a Gaussian-like oscillator.

The dielectric function in RLM is given by [28, 29]

$$\varepsilon(\omega) = \varepsilon_\infty + \sum_j \frac{F_j \mathrm{e}^{\mathrm{i}\beta_j}}{\omega_j^2 - \omega^2 - \mathrm{i}\Gamma'_j\omega}, \tag{4}$$

where j is the number of oscillators and ω_j, F_j, Γ'_j, and β_j are the peak frequency, strength, broadening, and phase factor of the jth oscillator, respectively.

It should be noted that in CLM the imaginary part of the optical function decays in the same way on both sides of a peak ($\omega > \omega_j$ and $\omega < \omega_j$). However, it was suggested that the MPcs may have asymmetrical peaks [20]. Asymmetry may exist on the higher and lower energy sides of the 1.98 eV peak of ZnPc as well as CuPc. Therefore, an asymmetrical model might be useful when fitting the SE data. To provide more freedom in choosing the shape of the absorption peak, we have proposed and tested an inherently asymmetrical model—DLM. The DLM is based on the classical Lorentz model. The parameter Γ in the CLM represents the width of the oscillator. In the proposed DLM, each oscillator has two Γ values, one for the lower energy side of the peak and the other one for the higher side. For each oscillator, the dielectric constant is assumed as below:

$$\varepsilon = \varepsilon_\infty + \begin{cases} \dfrac{F}{\omega^2 - \omega_0^2 + \mathrm{i}\Gamma_1\omega} & \omega < \omega_0, \\ \dfrac{F\Gamma_2}{\Gamma_1(\omega^2 - \omega_0^2 + \mathrm{i}\Gamma_2\omega)} & \omega \geqslant \omega_0, \end{cases} \tag{5}$$

where E_0 is the oscillator frequency, F is the oscillator strength, and Γ_1 and Γ_2 are the two widths. However,

detailed analysis shows that the above optical function is not consistent with the KK relation. In order to be consistent with the KK relation, only the imaginary part of the dielectric constant defined by the above equation is taken as the imaginary part of DLM, and the real part of DLM is calculated by KK inversion. A numerical KK inversion algorithm described in [34] was used. The fitting algorithm used for all models and point-to-point fitting was the simulated annealing algorithm.

We did not take into account surface roughness in modelling the data since no significant improvements were found with surface roughness correction when the data for films deposited on glass and Si substrates are fitted simultaneously. This is expected since AFM measurements of MPc films on quartz substrates revealed that the surface roughness was small, ∼2 nm for all five materials. However, since the surface roughness of MPc films is strongly dependent on the deposition conditions [35], it is always advisable to perform AFM measurements to examine the surface before attempting to fit the ellipsometry data. If the surface roughness of a MPc is large, surface roughness correction using Bruggeman effective medium approximation (EMA) [36] is needed [27]. When a model for the dielectric function is used, surface roughness correction is straightforward [27]. However, when point-by-point fitting is performed, it is possible that keeping the thickness of the rough layer as a fitting parameter would result in different thickness at different wavelengths. This problem can be resolved by setting the thickness of the rough layer to a value determined from AFM measurements. However, it is possible that the estimate of roughness from SE data and AFM would be different. It was shown that the ratio between the roughness estimates obtained by SE and AFM depends on the window size in the AFM scan [37]. Therefore, surface roughness correction needs to be performed carefully to ensure good results. For substrate temperatures higher than room temperature, it may also be necessary to take into account the existence of larger microcrystallites that do not have a spherical shape by fitting the depolarization factor q ($q = \frac{1}{3}$ in conventional EMA) [38].

4. Results and discussion

The optical properties of different MPcs, as observed from the absorption spectra reported in the literature and measured by us, are rather similar in the 250–800 nm spectral range. Four transitions can be identified in this range, and the locations of the peaks for different materials are very close, although the strengths and the broadening parameters vary. Unlike the other four materials, which have two transitions in the Q band, in the Q band of FePc, three transitions can be identified. The fitted parameters for different models are shown in tables 1–5, and the comparison between experimental and calculated $\tan\Psi$ and $\cos\Delta$ for films on glass and silicon substrates are shown in figures 1–5 for CoPc, CuPc, FePc, NiPc, and ZnPc, respectively. The RLM fitting result is not shown for clarity since for all materials the curves almost entirely overlap with either MLM or DLM. The agreement with the experimental data is the best for point-to-point fitting, followed by similar results obtained from MLM, DLM, and RLM, while the worst agreement is obtained by CLM. For some of the materials, such as FePc, the agreement with the experimental data is about equally good for all four oscillator models. No significant improvement can be obtained by increasing the number of oscillators. At least seven oscillators were used in [19], while only five oscillators were used in our study (six oscillators were used for FePc due to one additional transition in the Q band). From the fitted values of the broadening factor, α, in MLM, it can be observed that not all the peaks are Lorentzian, some of them are Gaussian-like, and some have wings that decay slightly faster than the wings of a Gaussian function. This is consistent with the results in [19, 31]. The Lorentz model results from homogeneous broadening mechanisms in which all molecules have the same transition energy and are subject to the same relaxation processes. Gaussian bands, on the other hand, arise from an inhomogeneous broadening mechanism in which the molecular transition energy is shifted on a random basis. While the individual transitions may be Lorentzian, the overall spectra are not necessarily in the exact Lorentz lineshapes.

The DLM can also achieve good fitting results but not better than MLM. Because the n, k values were obtained by interpolation, at the long wavelength side the curve is not smooth, but this problem can be solved by measuring the SE data with an equal frequency interval. The two fitted widths for an oscillator are not equal, which indicates that the oscillators are indeed asymmetrical. The RLM also obtains comparable results with MLM and DLM. For all modifications of the Lorentz model investigated here, the fitting results are superior to the CLM. However, no general recommendations other than

Table 1. The model parameters for the CLM, the RLM, the MLM, and the DLM for CoPc.

Model	CLM					RLM				
Parameter	ω (eV)	F (eV^2)	Γ (eV)	ε_∞		ω (eV)	F (eV^2)	Γ (eV)	β	ε_∞
osc. 1	1.79	0.59	0.19	1.6		1.78	0.68	0.21	0.094	1.43
osc. 2	2.01	1.06	0.24			2.01	1.06	0.24	0	
osc. 3	3.70	3.09	0.56			3.66	3.49	0.64	0.227	
osc. 4	4.33	5.03	0.83			4.34	4.38	0.87	0	
osc. 5	5.83	18.5	0.5			6.24	27.7	1	0.025	
Model	MLM					DLM				
Parameter	ω (eV)	F (eV^2)	Γ (eV)	a	ε_∞	ω (eV)	F (eV^2)	Γ_1 (eV)	Γ_2 (eV)	ε_∞
osc. 1	1.78	0.58	0.20	0.58	1.24	1.78	0.60	0.18	0.22	1.6
osc. 2	2.01	1.18	0.25	0		2.01	0.99	0.23	0.24	
osc. 3	3.68	2.23	0.53	0.58		3.68	3.63	0.56	1.2	
osc. 4	4.32	8.18	1.16	0		4.34	2.13	0.55	1.08	
osc. 5	6.24	30.0	1.27	1		5.96	14.8	0.61	1.17	

Table 2. The model parameters for the CLM, the RLM, the MLM, and the DLM for CuPc.

Model			CLM					RLM		
Parameter	ω (eV)	F (eV^2)	Γ (eV)	ε_∞		ω (eV)	F (eV^2)	Γ (eV)	β	ε_∞
osc. 1	1.78	0.40	0.15	1.39		1.76	0.64	0.20	0.134	1.00
osc. 2	2.00	1.28	0.24			2.00	1.36	0.25	0.074	
osc. 3	3.61	4.08	0.56			3.53	5.46	0.75	0.352	
osc. 4	4.66	2.34	0.80			4.64	1.51	0.60	0.288	
osc. 5	6.15	22.6	0.50			6.20	27.9	0.51	0.092	
Model			MLM					DLM		
Parameter	ω (eV)	F (eV^2)	Γ (eV)	a	ε_∞	ω (eV)	F (eV^2)	Γ_1 (eV)	Γ_2 (eV)	ε_∞
osc. 1	1.77	0.47	0.18	1.00	1.00	1.76	0.36	0.12	0.25	1.02
osc. 2	2.00	1.39	0.26	0.26		2.00	0.92	0.18	0.25	
osc. 3	3.62	4.84	0.65	0.10		3.51	2.87	0.42	1.06	
osc. 4	4.72	3.43	0.93	0.61		4.68	1.12	0.48	0.67	
osc. 5	6.20	29.7	0.84	0.92		6.20	19.8	0.5	1.46	

Table 3. The model parameters for the CLM, the RLM, the MLM, and the DLM for FePc.

Model			CLM					RLM		
Parameter	ω (eV)	F (eV^2)	Γ (eV)	ε_∞		ω (eV)	F (eV^2)	Γ (eV)	β	ε_∞
osc. 1	1.75	0.39	0.26	1.43		1.75	0.41	0.26	0.023	1.42
osc. 2	1.97	0.83	0.33			1.97	0.81	0.33	0	
osc. 3	2.20	0.65	0.10			2.20	0.06	0.10	0	
osc. 4	3.59	2.41	0.67			3.58	2.35	0.66	0.254	
osc. 5	4.27	7.75	1.46			4.27	7.95	1.49	0	
osc. 6	6.20	27.8	0.65			6.20	27.7	0.62	0	
Model			MLM					DLM		
Parameter	ω (eV)	F (eV^2)	Γ (eV)	a	ε_∞	ω (eV)	F (eV^2)	Γ_1 (eV)	Γ_2 (eV)	ε_∞
osc. 1	1.74	0.27	0.23	0.41	1.32	1.74	0.35	0.23	0.38	1.37
osc. 2	1.97	1.14	0.40	0		1.93	0.75	0.36	0.26	
osc. 3	2.20	0.03	0.06	0.62		2.21	0.15	0.19	0.08	
osc. 4	3.58	2.22	0.68	0		3.55	1.83	0.54	0.90	
osc. 5	4.22	8.13	1.50	0		4.31	8.74	1.76	1.36	
osc. 6	6.10	29.5	1.03	0.29		6.31	29.5	0.73	0.92	

Table 4. The model parameters for the CLM, the RLM, the MLM, and the DLM for NiPc.

Model			CLM					RLM		
Parameter	ω (eV)	F (eV^2)	Γ (eV)	ε_∞		ω (eV)	F (eV^2)	Γ (eV)	β	ε_∞
osc. 1	1.81	0.54	0.17	1.55		1.81	0.57	0.18	0	1.49
osc. 2	2.01	1.05	0.19			2.01	1.19	0.22	0	
osc. 3	3.58	2.04	0.51			3.58	2.80	0.64	0	
osc. 4	4.43	5.86	1.01			4.36	7.23	1.19	0.404	
osc. 5	6.07	21.0	0.50			6.20	17.6	0.50	0	
Model			MLM					DLM		
Parameter	ω (eV)	F (eV^2)	Γ (eV)	a	ε_∞	ω (eV)	F (eV^2)	Γ_1 (eV)	Γ_2 (eV)	ε_∞
osc. 1	1.80	0.42	0.17	0.82	1.04	1.79	0.26	0.10	0.16	1.73
osc. 2	2.00	1.36	0.24	0		2.02	1.71	0.32	0.18	
osc. 3	3.59	3.18	0.63	0		3.54	1.83	0.46	0.80	
osc. 4	4.45	5.71	0.96	1.00		4.46	5.25	0.94	1.20	
osc. 5	6.08	30.0	1.15	0.87		5.90	11.0	0.73	1.50	

Table 5. The model parameters for the CLM, the RLM, the MLM, and the DLM for ZnPc.

Model			CLM					RLM		
Parameter	ω (eV)	F (eV^2)	Γ (eV)	ε_∞		ω (eV)	F (eV^2)	Γ (eV)	β	ε_∞
osc. 1	1.77	0.92	0.24	2.14		1.76	0.89	0.25	0	1.51
osc. 2	2.00	0.98	0.21			2.00	1.43	0.29	0	
osc. 3	3.58	3.95	0.58			3.50	5.58	0.78	0.365	
osc. 4	4.37	2.16	1.00			4.50	1.01	1.00	0.188	
osc. 5	5.71	8.23	0.85			6.40	22.8	0.65	0	
Model			MLM					DLM		
Parameter	ω (eV)	F (eV^2)	Γ (eV)	a	ε_∞	ω (eV)	F (eV^2)	Γ_1 (eV)	Γ_2 (eV)	ε_∞
osc. 1	1.76	1.03	0.26	0	1.31	1.75	0.61	0.19	0.21	1.54
osc. 2	2.01	1.16	0.27	0.79		2.01	1.66	0.33	0.25	
osc. 3	3.58	5.28	0.73	0		3.52	3.84	0.54	1.19	
osc. 4	4.50	2.69	1.11	0.87		4.58	0.50	0.45	1.05	
osc. 5	6.39	30.0	1.30	0.96		6.21	15.0	0.68	2.00	

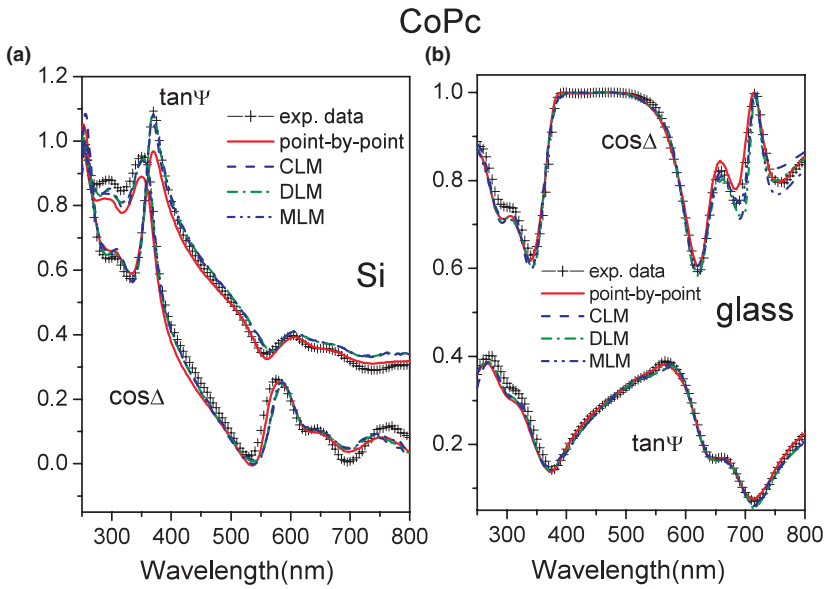

Figure 1. (*a*) Tan Ψ and cos Δ for CoPc film on Si substrate. (*b*) Tan Ψ and cos Δ for CoPc film on glass substrate. +, experimental data; ——, point-to-point fit; - - - -, CLM; — · —, DLM; and — · · —, MLM. The thickness is 48 nm.

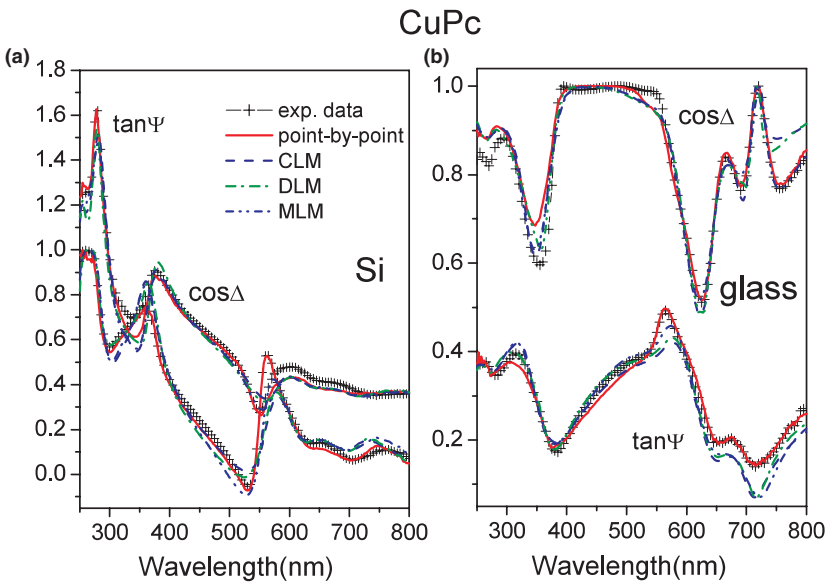

Figure 2. (*a*) Tan Ψ and cos Δ for CuPc film on Si substrate. (*b*) Tan Ψ and cos Δ for CuPc film on glass substrate. +, experimental data; ——, point-to-point fit; - - - -, CLM; — · —, DLM; and — · · —, MLM. The thickness is 49 nm.

that the CLM is inadequate for describing thin MPc films can be made since the performance of different modifications of the Lorentz model is similar. Unfortunately, unlike inorganic semiconductors, for which a variety of available models of optical functions exist, the choice of models for organic materials is very limited. Therefore, point-to-point fitting likely represents the best way to determine the optical functions, provided that the smoothness and continuity of the obtained optical functions are ensured. Due to possible multiple solutions, usually more reliable results are obtained from an overdetermined system, such as the fitting procedure used in this work. A modified Lorentz oscillator model can also achieve good agreement with the experimental results for all five MPcs, although the agreement is slightly worse than the point-to-point fitting. Due to its flexibility (i.e. adjustable broadening), this model can be recommended, provided that KK consistency is verified for large values of the α parameter [39].

Therefore, for fitting the optical functions of MPcs, either point-to-point fitting or some modification of the Lorentz model should be used, and in the case of a rough surface (which depends on the deposition conditions), it may be necessary to employ surface roughness correction. The unsuitability of the conventional Lorentz oscillator model is likely due to inherent inhomogeneous broadening contributions. Any kind of inhomogeneity, such as impurities, fluctuations of well width in

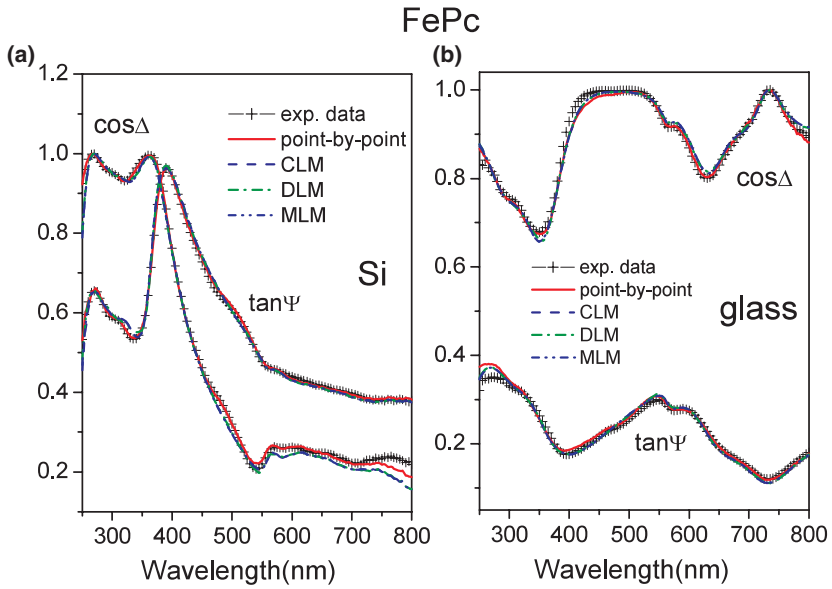

Figure 3. (*a*) Tan Ψ and cos Δ for FePc film on Si substrate. (*b*) Tan Ψ and cos Δ for FePc film on glass substrate. +, experimental data; ——, point-to-point fit; - - - -, CLM; — · —, DLM; and — · · —, MLM. The thickness is 56 nm.

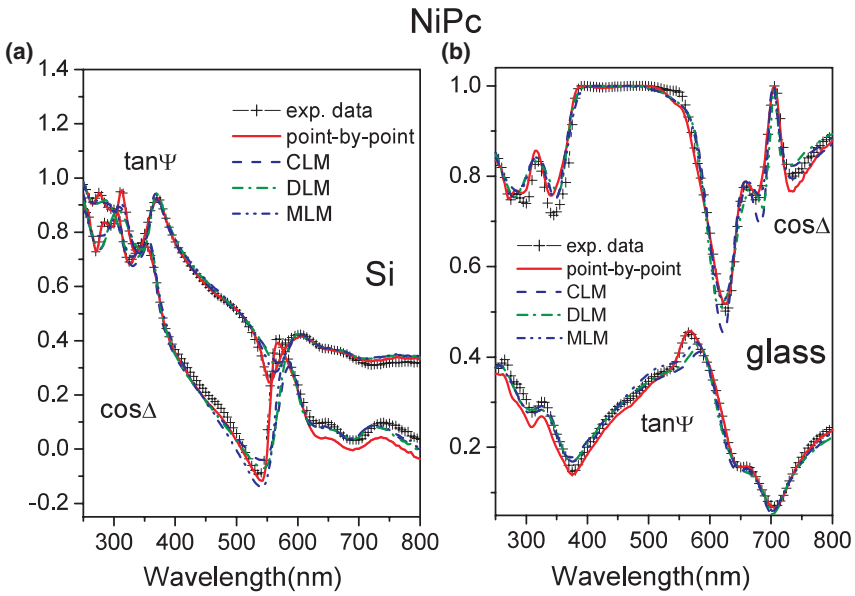

Figure 4. (*a*) Tan Ψ and cos Δ for NiPc film on Si substrate. (*b*) Tan Ψ and cos Δ for NiPc film on glass substrate. +, experimental data; ——, point-to-point fit; - - - -, CLM; — · —, DLM; and — · · —, MLM. The thickness is 45 nm.

quantum well structures, composition fluctuations, interfacial roughness, and non-periodicity, will give rise to Gaussian broadening [40, 41]. Since MPc films are polycrystalline, with grain size in the range 36–53 nm, depending on the deposition conditions [42], it is expected that there would be some inhomogeneous broadening. This is in agreement with the study of Franke *et al* [31]. Also, it should be pointed out that the broadening due to exciton–phonon interaction has a Lorentzian shape only in the central part of the absorption peak [43, 44]. The actual lineshape is inherently asymmetric [43] and assumes a symmetric form only if the energy dependence of the parameters is disregarded. The general symmetric lineshape of an exciton can assume a form from Gaussian to Lorentzian, depending on certain material-dependent parameters and the temperature [44]. Therefore, it is expected that the modifications of CLM that take into account the existence of inhomogeneous broadening and/or peak asymmetry would result in an improved fit of the experimental data.

The real and imaginary parts of the refractive index of CoPc, CuPc, FePc, NiPc, and ZnPc obtained are shown in figure 6. The extinction coefficient obtained is in agreement with the absorption spectra of CoPc, CuPc, and NiPc reported in [19] as well as the absorption spectra of CoPc, CuPc, FePc, and ZnPc reported in [20]. The complex refractive index of CuPc shows very good agreement with the data reported

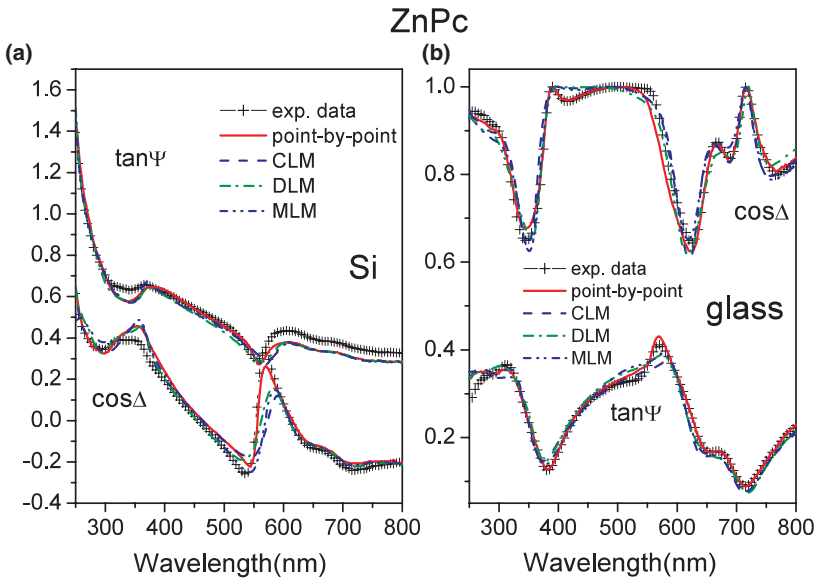

Figure 5. (*a*) Tan Ψ and cos Δ for ZnPc film on Si substrate. (*b*) Tan Ψ and cos Δ for ZnPc film on glass substrate. +, experimental data; ——, point-to-point fit; - - - -, CLM; — · —, DLM; and — · · —, MLM. The thickness is 36 nm.

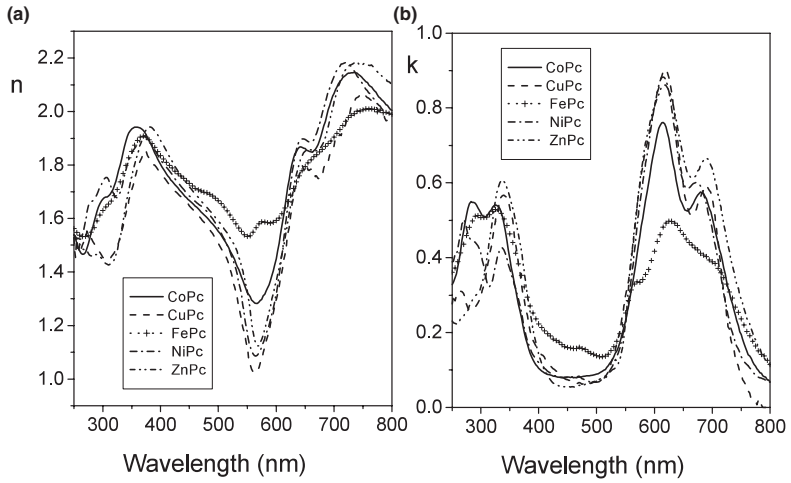

Figure 6. (*a*) The real part of the index of refraction of MPcs. (*b*) The imaginary part of the index of refraction of MPcs. ——, CoPc; - - - -, CuPc; +, FePc; — · —, NiPc; — · · —, ZnPc.

in [45]. Two peaks in the k spectrum reported in [45] can be identified, 0.9 at 620 nm and 0.6 at 695 nm, which are in excellent agreement with our data showing k peak values of 0.9 at 617.5 nm and 0.59 at 690 nm. For FePc, both our results and the absorption measurements by Davidson [20] show that there are three transitions in the Q band, which justifies the assignment of six oscillators for FePc. The results obtained are also in good agreement with the other studies reported in the [17, 18, 24] with the exception of the data reported by Gu and Chen [25, 26]. That may be due to the different thicknesses in their work: the CoPc film they studied had a thickness of 631.85 nm and the CuPc film had a thickness of 1579 nm, which is much greater than those used in this study. Furthermore, the shape of extinction coefficient obtained in their work is not in agreement with the absorption spectra reported in the literature.

MPcs have several polymoprhic forms, of which the two stable polymorphic crystalline forms, the α form and the β form, are the best known ones [17]. MPcs films sublimed at room temperature and a pressure less than 50 Torr are in the α form, while films sublimed at a high temperature (>300°C) or at a higher pressure are in the β form. α films can be changed into β films by annealing the films at above 300°C for several hours [46]. From the fabrication conditions and measured absorption spectra, the films studied here are most likely polycrystalline and in the α form [47]. In order to verify the crystallinity of the films, we performed x-ray diffraction (XRD) measurements using a Siemens D5000 x-ray diffractometer for 50 nm thick NiPc films. Figure 7 shows the results obtained. For films deposited on the glass substrate, the broad peak between 15° and 35° is due to the glass substrate. The results obtained are in excellent agreement with the previously reported results for NiPc films in the α form [6, 42, 48]. From XRD measurements, we determined the grain size to be ∼40 nm for the glass substrate and ∼37 nm for the Si substrate, which is in excellent agreement

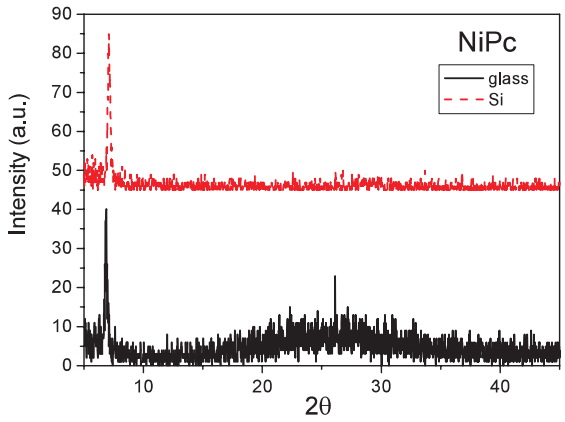

Figure 7. XRD spectra of 50 nm NiPc films on glass (——) and Si substrates (- - - -). The curves have been shifted vertically for clarity.

with previously reported studies for NiPc films deposited on unheated substrates [42, 48].

While each Pc molecule is expected to be anisotropic due to its planarity, overall anisotropy is not expected for entirely random molecular orientations. The important question is whether the stacking is truly random in polycrystalline MPc films deposited at room temperature on glass and Si substrates. From XRD measurements, it can be seen that some preferential stacking can be detected [42, 48]. Since the films are not perfectly ordered, however, the expected degree of anisotropy is not fully clear. We have found that the optical constants of MPcs are dependent on the film thickness. For each MPc, several batches of samples were fabricated, with decreasing thickness. It was found that only for films with thickness below ∼60 nm could satisfactory fitting with the isotropic sample model be obtained. It is possible that with increasing thickness either there is some preferential ordering

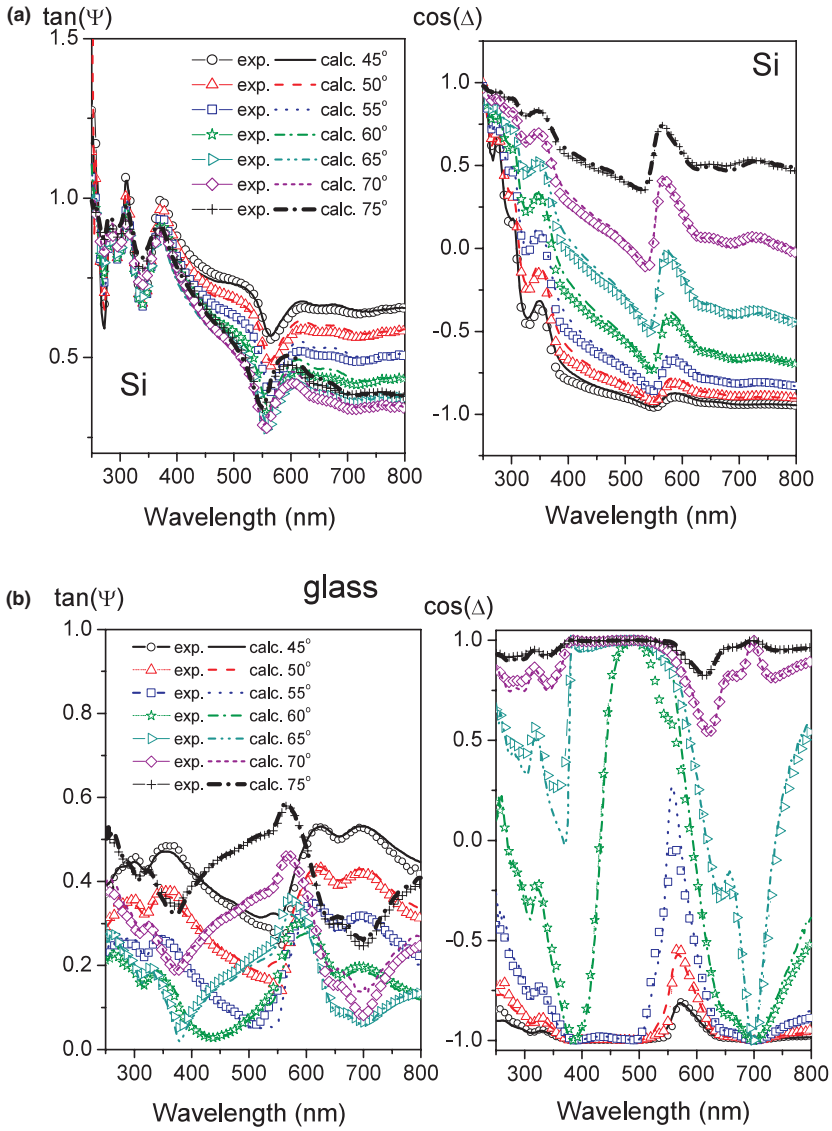

Figure 8. (*a*) Tan Ψ and cos Δ for NiPc film on Si substrate for different incident angles. (*b*) Tan Ψ and cos Δ for NiPc film on glass substrate for different incident angles. The thickness is 45 nm.

of crystallites causing anisotropy, or there are differences in the ordering of crystallites on the glass substrates and Si substrates, so that the measured SE data with glass substrates and Si substrates could not be fitted simultaneously. This is in agreement with the results of Barrett *et al* [22], who found that thin (<80–100 nm) CuPc films can be described with an isotropic model, while for thicker films anisotropy needs to be taken into account. In their study, it was found that the deposited film consisted of small crystallites with random orientation in the plane of film. As the film thickness grows, the crystallites grow and become more closely packed, which results in anisotropy. It was suggested that for MPc films less than 100 nm thick, isotropic models are suitable, and for films larger than 100 nm, anisotropic models are needed. In our study, MPc films with thicknesses larger than 60 nm could not be fitted by the isotropic model.

In order to verify whether the samples with thickness below 60 nm are truly isotropic, we also performed the ellipsometry measurements for NiPc samples at different incident angles. Seven incident angles were tested: 45°, 50°, 55°, 60°, 65°, 70°, and 75°. All the SE data were fitted point-by-point with the same n and k and the same thickness. The success of the fitting, combined with the comparison of the four sets of data for each sample, verified the isotropy or the insignificance of the anisotropy of NiPc films (figure 8). The fitting result is slightly worse for glass substrates than for Si substrates. There are several possible reasons for this. One possible reason is the calibration variation: calibrations for samples on glass substrates are usually more difficult than those for samples on Si substrates, due to the weaker signals, and so the SE data measured for samples on glass substrates are not as accurate as for samples on Si substrates. Another possible reason is a higher surface roughness of the films deposited on glass substrates. In order to verify this assumption, AFM measurements were performed. The AFM result confirms a higher roughness of the samples deposited on glass substrates, which is expected due to the higher roughness of the substrate itself (i.e. glass substrates are more rough than Si wafers).

5. Conclusions

We have performed SE measurements of thin films of five MPcs: CoPc, CuPc, FePc, NiPc, and ZnPc. The optical functions of MPcs were extracted using point-to-point fitting, the conventional Lorentz oscillator model, the modified Lorentz oscillator model, the RLM, and the DLM. The data for the films deposited on Si and glass substrates were fitted simultaneously. While all the modifications of the Lorentz model performed better compared with the CLM, the performance of the different modifications is rather similar. Therefore, the only definite conclusion that can be drawn is that MPc thin films cannot be adequately described with pure Lorentzian oscillators. The isotropic model was sufficient for the films with thickness below 60 nm, which is in agreement with previous reports in the literature on CuPc. The validity of the isotropic model was verified by performing measurements for different incident angles. The measured spectra of films on Si and glass substrates for incident angles from 45° to 75° can be fitted successfully with the isotropic model, indicating that if there is any anisotropy in these films it is negligible for sufficiently thin samples.

References

[1] Leznoff C C and Lever A B P 1989 *Phthalocyanines: Properties and Applications* (New York: VCH)
[2] Guillaud G, Simon J and Germain J P 1998 *Coord. Chem. Rev.* **178–180** 1433
[3] Kobayashi N 2002 *Bull. Chem. Soc. Japan* **75** 1
[4] Peumans P and Forrest S R 2001 *Appl. Phys. Lett.* **79** 126
[5] Peumans P, Uchida S and Forrest S R 2003 *Nature* **425** 158
[6] Anthopoulos T D and Shafai T S 2003 *Appl. Phys. Lett.* **82** 1628
[7] Kaneko M, Taneda T, Tsukagawa T, Kajii H and Ohmori Y 2003 *Japan. J. Appl. Phys.* **42** (part I) 2523
[8] Xiao K, Liu Y, Yu G and Zhu D 2003 *Appl. Phys.* A **77** 367
[9] Mori T, Mitsuoka T, Ishii M, Fujikawa H and Taga Y 2002 *Appl. Phys. Lett.* **80** 3895
[10] Qiu Y, Gao Y D, Wei P and Wang L D 2002 *Appl. Phys. Lett.* **80** 2628
[11] Flora W H, Hall H K and Armstrong N R 2003 *J. Phys. Chem.* B **107** 1142
[12] Newton M I, Starke T K H, Willis M R and McHale G 2000 *Sensors Actuators* B **67** 307
[13] Spadavecchia J, Ciccarella G, Rella R, Capone S and Siciliano P 2003 *Sensors Actuators* B **96** 489
[14] Edwards L and Gouterman M 1970 *J. Mol. Spectrosc.* **33** 292
[15] Eastwood D, Edwards L, Gouterman M and Steinfeld J 1966 *J. Mol. Spectrosc.* **20** 381
[16] Huang T H and Sharp J H 1982 *Chem. Phys.* **65** 205
[17] Lucia E A and Verderame F D 1968 *J. Chem. Phys.* **48** 2674
[18] Schechtman B H and Spicer W E 1970 *J. Mol. Spectrosc.* **33** 28
[19] Hollebone B R and Stillman M J 1978 *J. Chem. Soc. Faraday Trans.* II **74** 2107
[20] Davidson A T 1982 *J. Chem. Phys.* **77** 168
[21] Laurs H and Heiland G 1987 *Thin Solid Films* **149** 129
[22] Barrett M A, Borkowska Z, Humphreys M W and Parsons R 1975 *Thin Solid Films* **28** 289
[23] Debe M K and Field D R 1991 *J. Vac. Sci. Technol.* A **9** 1265
[24] Debe M K 1992 *J. Vac. Sci. Technol.* A **10** 2816
[25] Gu D and Chen Q 1994 *Opt. Commun.* **110** 576
[26] Chen Q, Gu D and Gan F 1995 *Physica* B **212** 189
[27] Djurišić A B, Kwong C Y, Lau T W, Guo W L, Li E H, Liu Z T, Kwok H S, Lam L S M and Chan W K 2001 *Opt. Commun.* **205** 155
[28] Arwin H, Mårtensson J and Jansson R 1992 *Appl. Opt.* **31** 6707
[29] Mårtensson J and Arwin H 1991 *Thin Solid Films* **205** 252
[30] Masenelli B, Callard S, Gagnaire A and Joseph J 2000 *Thin Solid Films* **364** 264
[31] Franke A, Stendal A, Stenzel O and von Borczyskowski C 1996 *J. Opt. A: Pure Appl. Opt.* **5** 845
[32] Vincett P S, Voigt E M and Rieckhoff K E 1971 *J. Chem. Phys.* **55** 4131
[33] Chahraoui D, Valat P and Kossanyi J 1992 *Res. Chem. Intermed.* **17** 219
[34] Ohta K and Ishida H 1988 *Appl. Spectrosc*. **42** 952
[35] Grządziel L, Żak J and Szuber J 2003 *Thin Solid Films* **436** 70
[36] Tompkins H G 1993 *A User's Guide to Ellipsometry* (Boston: Academic) pp 246–51
[37] Petrik P, Lohner T, Fried M, Biro L P, Khanh N Q, Gyulai J, Lehnert W, Schneider C and Ryssel H 2000 *J. Appl. Phys.* **87** 1734
[38] Logothetidis S 1989 *J. Appl. Phys.* **65** 2416
[39] Schubert M, Woollam J A, Leibiger G, Rheinländer B, Pietzonka I, Saß T and Gottschalch V 1999 *J. Appl. Phys.* **86** 2025

[40] Shields A J, Klipstein P C and Apsley N 1989 *Semicond. Sci. Technol.* **4** 476
[41] Arena C, Rotelli B and Tarricone L 1994 *Phys. Status Solidi* b **185** 505
[42] Narayanan Unni K N and Menon C S 2000 *Mater. Lett.* **45** 326
[43] Toyozawa Y 1964 *J. Phys. Chem. Solids* **25** 59
[44] Sumi H and Toyozawa Y 1971 *J. Phys. Soc. Japan.* **31** 342
[45] Fritz T, Hahn J and Böttecher H 1989 *Thin Solid Films* **170** 249
[46] Prabakaran R, Kesavamoorthy R, Reddy G L N and Xavier F P 2002 *Phys. Status Solidi* b **229** 1175
[47] Hassan A K and Gould R D 1992 *Phys. Status Solidi* a **132** 91
[48] Anthopoulos T D and Shafai T S 2003 *Thin Solid Films* **441** 207